


# DESIGN, MANUFACTURING, AND TESTING OF HUMPBACK WHALE-INSPIRED TUBERCLES FOR ENHANCED LOW-REYNOLDS WING PERFORMANCE.

E. Barroso[1], R. Bardera[2], J.C. Matías[3], J. Fernández[4] & A.A. Rodríguez-Sevillano[5]

[1,2,3,4] Instituto Nacional de Técnica Aeroespacial (INTA), Torrejon de Ardoz, Madrid, 28850, Spain
[5]Escuela Técnica Superior de Ingeniería Aeronáutica y del Espacio (ETSIAE-UPM), Madrid, 28040, Spain

## Abstract

This paper presents an experimental wind tunnel study on the aerodynamic behavior of several bioinspired wing configurations applied to a fixed-wing Small Remotely Piloted Aircraft System (RPAS). The vehicle, specifically designed and manufactured to operate at low Reynolds numbers, features a conventional configuration with a rectangular wing and a V-tail. The study is focused on the aerodynamic advantages associated with the leading-edge tubercles found on the pectoral fins of humpback whales, which have been widely reported to delay stall onset, increase lift force at high angles of attack, and improve aerodynamic performance under low-speed flight conditions.

Building on these characteristics, the application of bioinspired geometries to small RPAS wings has been investigated with the aim of enhancing aerodynamic efficiency, improving lift generation, and delaying flow separation. Several leading-edge tubercle configurations were designed, modeled in 3D, and tested in a low-speed wind tunnel. In a first stage, an idealized geometry with constant amplitude and wavelength along the wingspan was generated, corresponding to a regular sinusoidal leading edge. Subsequently, a more realistic bioinspired configuration was developed by introducing variable amplitude and wavelength, together with positive leading-edge sweep, in order to more closely reproduce the morphology of the humpback whale fin.

The results were compared against a base rectangular wing, allowing the influence of leading-edge tubercles on lift, drag, aerodynamic efficiency, and stall behavior to be assessed. The experimental results show that, although the base wing provides better performance at low angles of attack, the bioinspired configurations significantly improve the aerodynamic behavior near stall and post-stall conditions. The conventional wing stalls at approximately $10°$, whereas the constant tubercled wing delays stall up to around $15°$and the realistic humpback whale-inspired configuration up to approximately $16°$, corresponding to stall-delay improvements of about 5 and 6 degrees, respectively. At $12°$, the lift coefficient increases by approximately 11 % for the constant tubercled wing and 9 % for the realistic configuration, while the aerodynamic efficiency improves by approximately 11 % and 20 %, respectively. These results confirm the potential of leading-edge tubercles as a passive flow-control strategy to improve the aerodynamic performance of small RPAS operating at low Reynolds numbers.

**Keywords:** Bioinspiration, Humpback whale fin, RPA, Tubercles, Wind tunnel.

## 1. Introduction

Small remotely piloted aircraft (RPAs) operate in a particularly demanding aerodynamic regime due to their reduced dimensions and low flight speeds. Under these conditions, the Reynolds number is usually within a range in which viscous effects, laminar-turbulent transition, and the formation of laminar separation bubbles have a dominant influence on the aerodynamic behavior of the wing. In particular, the laminar separation bubble can significantly modify the pressure distribution over the airfoil, reduce lift force, increase aerodynamic drag, and promote an abrupt stall condition or stall with hysteresis. This phenomenon is especially critical in small vehicles, since it limits their ability to operate efficiently at low speed, during maneuvers with high angles of attack, or in the presence of vertical gusts.

In this context, passive flow control techniques are especially attractive, since they allow the structure of the boundary layer to be modified without the need for active systems, actuators, additional energy consumption, or complex mechanisms. One of the bioinspired solutions that has generated the greatest interest in recent decades is the incorporation of leading-edge tubercles, inspired by the protuberances present on the pectoral fins of the humpback whale. The literature has associated these structures with the high maneuverability of this animal, especially during tight feeding maneuvers, in which the fin must maintain lift at high angles of attack. Fish and Battle [1] identified the particular geometry of these fins as a possible hydrodynamic adaptation, and subsequent studies have related the tubercles to separation control mechanisms, generation of streamwise vorticity, and stall delay. Fish and Lauder [2] also discussed the relevance of biological flow-control mechanisms in swimming animals and their potential transfer to engineering applications. In addition, Fish et al. [3] reviewed the technological application of humpback whale tubercles, emphasizing their potential as a passive bio-inspired flow-control device. More recently, New and Ng [4] compiled a comprehensive overview of the morphology, aerodynamics, hydrodynamics, and applications of bio-inspired leading-edge tubercles.



Figure 1 – Humpback whale fin (Megaptera novaeangliae): breaching humpback whale showing relative size of the fin (left) and leading edge tubercles (right) [2].

The first experimental studies demonstrated that the modification of the leading edge by means of tubercles could substantially alter stall behavior. Miklosovic et al. [5] observed that the incorporation of tubercles on an idealized model of a humpback whale flipper delayed the stall angle by approximately 40 %, in addition to increasing lift and reducing drag. Johari et al. [6] analyzed the effect of tubercle amplitude and wavelength on a NACA 63-021 airfoil at low Reynolds number, showing that, although there could be a penalty in the pre-stall region, the modified configuration achieved lift values up to 50 % higher than the base airfoil in the post-stall regime. Hansen et al. [7] also pointed out that tubercles can act in a similar way to conventional vortex generators, modifying the structure of the boundary layer and the development of separation. Likewise, Zhang et al. [8] showed that leading-edge protuberances can be used as an aerodynamic control mechanism at low Reynolds numbers, while Rostamzadeh et al. [9] investigated the formation mechanism and influence of streamwise vortices generated by undulating leading-edge modifications.

Despite these benefits, the effect of tubercles is not universal and depends notably on the wing geometry, the airfoil used, the Reynolds number, the amplitude, the wavelength, and the spatial distribution of the protuberances. Various studies have indicated that wings with tubercles may present a certain reduction in performance in the pre-stall region, especially in terms of maximum lift or drag, while the improvements are usually clearer near stall and in the post-stall regime. This duality has been reported in different experimental and numerical investigations, where it is noted that tubercles may degrade behavior at low angles of attack, but improve post-stall lift, smooth stall and, in some cases, reduce aerodynamic drag once the stall angle of the conventional wing has been exceeded [6,7,10,11]. Therefore, the design of the bioinspired geometry must be carried out according to the specific application and the operating regime of the vehicle.

In the specific field of small RPAs, interest in this type of solution is due to the fact that these vehicles require high aerodynamic efficiency, stability, and recovery capability under non-stationary flight conditions or in the presence of gusts. Sudhakar et al. [12] carried out an experimental study on a high-aspect-ratio vehicle with two tubercle configurations: one with constant amplitude and wavelength, and another with variable parameters along the span. Their results showed that, at $Re = 0.18 \times 10^6$, the modified wings increased maximum lift, delayed stall, and reduced drag compared with the baseline wing, in addition to eliminating the hysteresis observed in the conventional configuration. In particular, the configuration with variable amplitude and wavelength presented better performance than the regular sinusoidal configuration, suggesting that a distribution more adapted to the wing geometry may be beneficial for real RPA applications. Other low-Reynolds-number studies, such as those of Sudhakar and Karthikeyan [13], also reported that sinusoidal leading-edge modifications can alter the pressure recovery and generate complex spanwise flow structures over conventional airfoils.

Other works have reinforced the importance of studying more realistic geometries and not limiting the analysis only to ideal sinusoidal tubercles. Moscato et al. [11] experimentally analyzed biomimetic wings with different tubercle geometries, observing that simplified leading-edge modifications can provide aerodynamic benefits while maintaining ease of manufacturing. Wei et al. [14] studied swept and tapered wings with tubercles, showing that these modifications can improve stall behavior and generate complex vortical structures over the wing surface, although they may also penalize efficiency in certain intermediate ranges of angle of attack. Murray et al. [15] also investigated the effect of leading-edge tubercles on swept wings, reporting that the performance enhancement associated with tubercles can remain relevant in three-dimensional swept configurations. Similarly, Seyhan et al. [16] analyzed a tapered swept-back SD7032 airfoil at low Reynolds number and found that leading-edge tubercles can significantly improve the lift curve over a wide range of angles of attack. Weber et al. [17] extended the application of tubercles to hydrodynamic lifting surfaces, studying their effect on lift, drag, and cavitation onset on rudders [18].

In addition to experimental studies, numerical approaches have contributed to understanding the aerodynamic mechanisms associated with tubercled leading edges. Ni et al. [10] proposed an empirically based model for predicting lift coefficients of twisted airfoils with leading-edge tubercles and compared the model with CFD results, providing further insight into stall behavior and the underlying flow mechanisms. Custodio [19] also contributed to the understanding of humpback whale-like leading-edge protuberances through hydrofoil studies, supporting the interpretation of tubercles as flow-control devices capable of modifying separation patterns.

In previous works applied to a small RPA with a rectangular wing with the effect of different sinusoidal tubercle configurations has been numerically analyzed using CFD. These results showed that the modified wings could increase lift in the post-stall regime and delay separation compared with the

baseline configuration. In particular, the configuration with the greatest amplitude and shortest wavelength achieved an increase of up to 17 % in the maximum lift coefficient and delayed stall up to an angle of attack of $20°$compared with the conventional case [20]. However, experimental validation of this type of solution remains necessary, especially when applied to a complete vehicle or to geometries specifically manufactured to operate under real low-Reynolds-number conditions.

The present work addresses this need through an experimental wind tunnel study of three wing configurations applied to a small RPA specifically designed and manufactured for this purpose. The base configuration corresponds to a rectangular wing and V-tail. On this geometry, two bioinspired configurations have been developed. The first incorporates a regular sinusoidal leading edge, defined by a constant amplitude and wavelength along the span. The second aims to approximate more closely the real morphology of the humpback whale fin, incorporating variable-size tubercles together with positive sweep of the leading edge. In the three configurations, the wing area has remained constant, so that the differences observed in lift force, aerodynamic drag, and aerodynamic efficiency can be mainly attributed to the geometric modification of the leading edge.

The main objective of this paper is to experimentally evaluate the influence of these bioinspired configurations on the aerodynamic characteristics of the small RPA, paying special attention to behavior at high angles of attack, stall delay, the evolution of maximum lift, and aerodynamic drag. To this end, wind tunnel tests have been carried out using a two-component external balance, capable of measuring lift and drag forces under the different flight conditions analyzed. The results obtained will allow a direct comparison between the conventional configuration and two levels of bioinspired complexity: an idealized sinusoidal geometry and a geometry closer to the natural distribution of tubercles observed in the humpback whale. This comparison is relevant not only from a scientific point of view, but also from a design perspective, since it makes it possible to assess whether the increase in geometric complexity associated with a more realistic bioinspired configuration translates into significant aerodynamic improvements for small RPAs.

## 2. Prototypes

### 2.1 Small RPA

As stated in the introduction, the primary aim of this paper is to evaluate and compare the aerodynamic behaviour of three different wings under low-Reynolds-number conditions, with a view to their possible application in small RPAs. The base configuration used as a reference corresponds to a small RPA previously developed through a collaboration between the National Institute for Aerospace Technology (INTA) and Technical University of Madrid (ETSIAE-UPM).

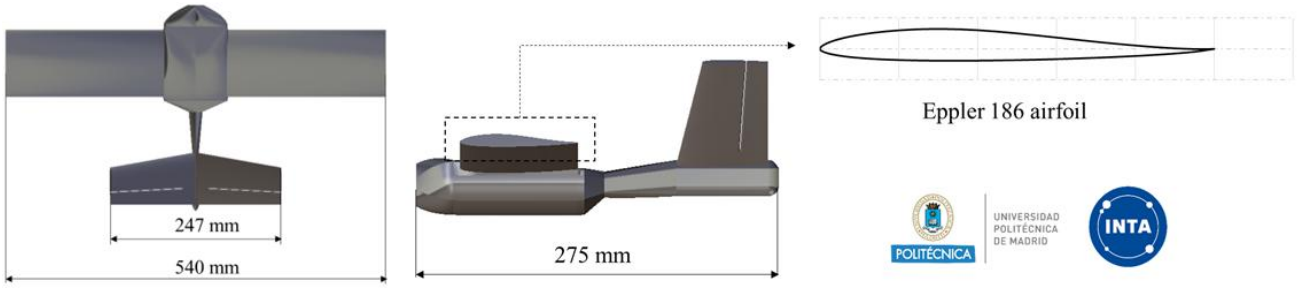



Figure 2 – Small RPA designed between INTA and UPM [14].

This reference vehicle features a rectangular wing planform and a V-tail. In its original configuration, the wing is equipped with Eppler 186 airfoils, while the V-tail employs NACA 0012 airfoils. The main geometric parameters of the model are presented in Figure 2. The vehicle has an overall length of 275 mm, a wingspan of 540 mm, and a wing chord of 90 mm [14].

## 2.2 Bioinspired configurations

Two bio-inspired wing configurations were designed and analyzed in this work in order to evaluate the aerodynamic influence of leading-edge tubercles on a small RPAS wing. Both configurations were developed from the same aerodynamic basis as the reference wing, using the conventional Eppler 186 airfoil along the span direction. This was decided on allowing the comparison to focus specifically on the effect of modifying the wing planform and the leading-edge geometry, rather than on changes associated with the airfoil section itself. In addition, the wing area was remained constant for the base and both bioinspired configurations, ensuring that the aerodynamic coefficients and force measurements could be compared in a direct way.

The inspiration for these configurations came from the pectoral fins of humpback whales, which possess characteristic tubercled leading edges. These natural protuberances are thought to contribute to lift enhancement during prey-capturing maneuvers, allowing the animal to perform sharp directional changes without a significant loss of lift. A considerable number of studies have confirmed the aerodynamic advantages of this type of geometry, particularly its ability to delay stall, improve post-stall behavior, and enhance lift generation at high angles of attack. Over the past decade, extensive research has therefore been devoted to leading-edge modifications incorporating tubercles, mainly due to their potential as passive flow-control devices [4 - 8]. The available literature includes a wide range of experimental and computational studies aimed at quantifying aerodynamic performance improvements and understanding the underlying flow-control mechanisms responsible for these effects.




Figure 3 – Several configurations: base wing (Base-W), constant tubercles on the wing (Tubercled-W) and realistic humpback whale fin (H.whale-W) and tubercles on a real wahle fin (right).

The first bioinspired configuration corresponds to an idealized tubercled wing. This geometry maintains the rectangular planform of the base wing but modifies the leading edge by introducing a sinusoidal distribution of tubercles (Tubercled-W). In this case, both the amplitude and the wavelength remain constant along the entire wingspan. Therefore, the leading edge follows a regular periodic function, producing equally spaced protuberances and troughs. This configuration represents a simplified bioinspired approach, commonly used in the literature to study the basic aerodynamic effect of leading-edge tubercles under controlled geometric conditions (see Figure 3).

To replicate the flow-control mechanisms observed in the pectoral fins of humpback whales, the rectangular wing geometry was modified to include sinusoidal tubercles along the leading edge. The leading-edge contour was mathematically described by a sinusoidal function with constant amplitude and wavelength.

The present work considers one idealized tubercled leading-edge configuration, defined by an amplitude of $a = 0.05c$ and a wavelength of $\lambda = 0.25c$. This particular set of parameters was selected based on prior analyses, which identified it as the configuration yielding the highest maximum lift coefficient among the tested geometries [14]. The regularity of this configuration makes it possible to

isolate the influence of a sinusoidal leading-edge modification while preserving the general rectangular layout of the original RPAS wing. Thus, this model provides a controlled geometry with which to assess the aerodynamic effect of constant-amplitude and constant-wavelength tubercles in comparison with the conventional base wing.

The second bioinspired configuration was designed to provide a more realistic biomimetic representation of the humpback whale fin. Unlike the idealized tubercled wing, this configuration does not use a uniform sinusoidal pattern along the span. Instead, the planform was defined following the geometry of a real humpback whale pectoral fin more closely, introducing variable-amplitude and variable-wavelength tubercles along the leading edge.

In this realistic configuration, larger tubercles are located close to the plane of symmetry, while smaller tubercles are progressively distributed toward the wing tip. This arrangement is intended to reproduce the natural morphology observed in humpback whale fins, where the tubercles are not identical but vary in size along the span direction. Furthermore, this configuration incorporates a positive leading-edge sweep angle of $10°$, while maintaining a straight trailing edge. As a result, the planform departs from the purely rectangular geometry of the base wing and becomes closer to the natural shape of a humpback whale fin.

This second configuration is particularly relevant because it allows the analysis to move beyond an idealized sinusoidal representation and toward a more biomimetic geometry. Therefore, it provides information about whether a more realistic tubercle distribution, inspired directly by the morphology of the animal, may offer additional aerodynamic benefits for small RPAS applications.

The comparison between these two bioinspired configurations makes it possible to assess the influence of different levels of geometric idealization. The sinusoidal tubercled wing represents a simplified and regular design, with constant amplitude and wavelength, whereas the realistic humpback whale-inspired wing introduces variable tubercle dimensions and leading-edge sweep in order to better approximate the natural biological geometry. By comparing both configurations with the conventional rectangular Eppler 186 wing, the study aims to determine whether these planform modifications can provide aerodynamic advantages for small RPAS applications, particularly in terms of lift generation, drag behavior, aerodynamic efficiency, and stall characteristics at low Reynolds numbers.

Maintaining the same wing area in all configurations is a key aspect of the experimental design. Since lift and drag forces are directly related to the reference area used to compute the aerodynamic coefficients, preserving the same area avoids misleading comparisons and ensures that the observed differences are mainly associated with the leading-edge and planform modifications. Therefore, any improvement or penalty in aerodynamic performance can be attributed to the incorporation of tubercles and to the degree of biomimetic realism introduced in the wing geometry.

## 3. Experimental Set-up

### 3.1 Wind tunnel

The experimental tests were carried out in the INTA low-speed wind tunnel, model Wk 860060-E, manufactured by Westenberg Engineering. This facility is an open circuit wind tunnel equipped with a closed circular test section measuring 600 mm in diameter and 1200 mm in length. The wind tunnel provides a flow with a turbulence intensity lower than 0.5 %, while the freestream velocity can be regulated up to 60 m/s through a frequency-controlled drive system.

### 3.2 Manufacturing process

The prototypes used in this study were manufactured using 3D printing at INTA's facilities. Due to the limited dimensions of the available machines, each semi-model was divided into three main modules (as seen in previous section): fuselage, wing, and tail.

The fuselage and tail were manufactured in PLA using 3D printing, since these components have a

less demanding geometry and mainly require stiffness, low weight, and ease of manufacturing. In contrast, the different wings were manufactured using resin 3D printing, due to the greater geometric complexity of the analysed configurations and the need to accurately reproduce both the leading-edge tubercles and the sharp trailing edge of the airfoil.

Resin manufacturing made it possible to obtain a high-quality surface finish, with low roughness and good geometric definition. This aspect is especially important in aerodynamic tests, since surface roughness can influence the behaviour of the boundary layer and, consequently, the forces measured during the test (see Figure 4).



Figure 4 – Details of the manufacturing process.

Due to the reduced build volume of the resin printer, each wing was manufactured in two sections. Both parts were then joined using two metallic inserts, which were used to ensure the correct alignment of the two halves and to provide structural stiffness to the joint (see detail in Figure 3). This solution made it possible to obtain wings that were resistant, lightweight, and suitable for withstanding the loads generated during wind tunnel testing.

The manufacturing methodology employed allowed the prototypes to be produced in a short time and at low cost, facilitating the experimental comparison between the three wing configurations: the conventional wing (rectangular), the humpback whale-inspired wing, and the constant tubercled wing.

The models were manufactured in a vertical orientation, so that the layer-by-layer build direction was aligned along the spanwise direction of the wing. This printing approach was selected to ensure that the printed layers were oriented parallel to the freestream velocity during wind tunnel testing. As a result, potential surface roughness effects were minimized, reducing the risk of inducing premature flow separation due to manufacturing related surface irregularities. As a final step in the surface finishing process, a thin layer of black paint was applied to the model surface in order to obtain a fully smooth and uniform finish.

### 3.3 Experimental tests

A two-component external force balance was employed to determine the aerodynamic loads during the wind tunnel tests. This external balance was specifically designed, manufactured, and calibrated at INTA's facilities for experiments with small RPAS.

The system consists of two 1 kg load cells, used to measure lift and aerodynamic drag forces, which are installed at opposite ends of a metallic support plate, as shown in Figure 4.

When the balance is aligned with the Z-axis, the aerodynamic forces generated by the model act within the X–Y plane. The loads transferred from the model to the balance produce bending deformation in the sensors. The deformation associated with the X-direction is used to determine the aerodynamic drag, measured by the 2-LC sensor, whereas the deformation in the Y-direction provides the lift measurement, obtained from the 1-LC sensor (see Figure 5).

During the experimental tests, the external balance was positioned below the models so that the

prototype and the measuring system behaved as a single rigid assembly. This arrangement ensured that the reference axes of the model and the balance remained correctly aligned throughout the measurements.

For each angle of attack, the voltage signals corresponding to lift and drag masures were acquired simultaneously over a period of 10 s. The sampling frequency was set to 100 Hz, resulting in a total of 1000 evenly spaced samples for each tested configuration and angle of attack.

All tests were conducted at a Reynolds number of $Re = 7.2 \times 10^4$. This value is representative of the typical operating regime of small RPAs and corresponds to a freestream velocity of aproximatelly $10$ m/s. The angle of attack, $\alpha$, was varied systematically from $-5°$to $+20°$, using increments of $1°$between consecutive test points.

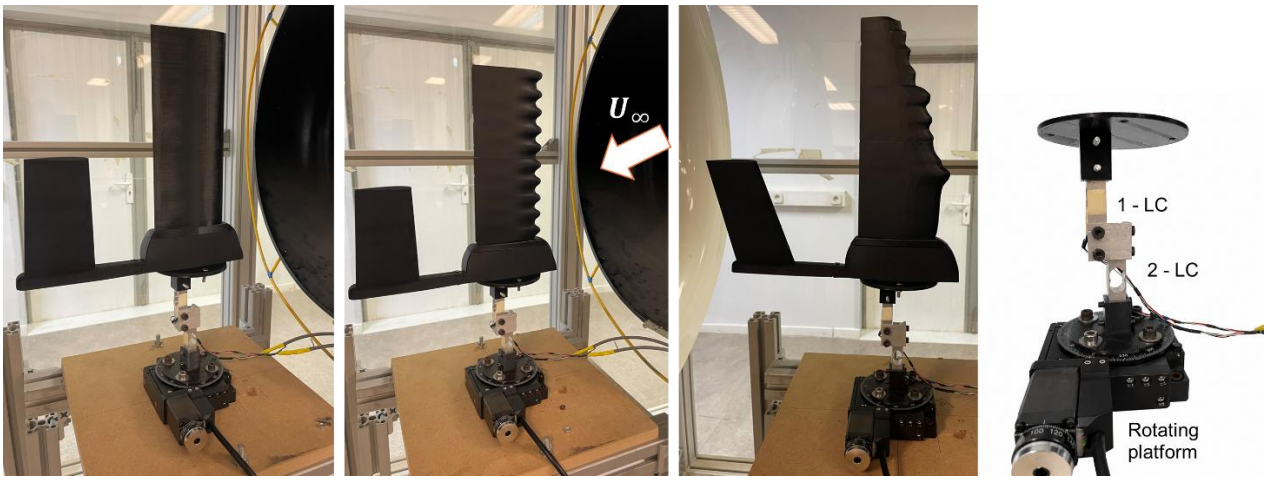



Figure 5 – Experimental tests.

## 4. Analysis of results

### 4.1 Lift coefficient

At low angles of attack, the Eppler 186 wing shows the highest lift coefficient values. In particular, in cruise configuration, that is, at an angle of attack of $0°$, the $C_L$ of this wing configuration is approximately 20 % higher than that obtained with the bioinspired configurations (see Figure 6).

However, this difference progressively decreases as the angle of attack increases. For angles of attack between approximately $5°$and $7°$, the advantage of the conventional wing (Eppler 186 airfoil) is reduced to values close to 5 %. In the range between $7°$and $10°$, the difference becomes even smaller, reaching approximately 2 – 3 %.

The conventional wing reaches its maximum lift coefficient at around $10°$, with an approximate value of $C_{L,\max} \approx 0.74$. Beyond this angle of attack, the conventional configuration enters stall, and a degradation of the lift coefficient is observed.

In contrast, the two bioinspired configurations maintain a more favourable $C_L$ evolution for angles of attack above $10°$.

At an angle of attack of $12°$, the humpback whale-inspired wing shows a $C_L$ approximately 9% higher than that of the conventional wing (Eppler 186), while the constant tubercled wing achieves an increase of approximately 11%.

For higher angles of attack, the differences become even more significant. In this regime, the bioinspired configurations provide lift increases of approximately 17 – 25% compared with the conventional wing, with the constant tubercled wing showing slightly higher values.

One of the most relevant results is the delay of stall condition. While the conventional wing stalls at approximately $10°$, the constant tubercled configuration delays this phenomenon up to around $15°$, corresponding to an increase of approximately 5 degrees. The realistic humpback whale-inspired configuration delays stall up to approximately $16°$, representing an improvement of around 6 degrees compared with the conventional wing.

Therefore, although the conventional wing provides slightly higher lift in the linear regime and at low angles of attack, the bioinspired configurations show a more robust behaviour near and beyond stall. This indicates that leading-edge tubercles allow the operational range of the wing to be extended, maintaining high lift values at angles of attack where the conventional wing has already started to lose aerodynamic performance.

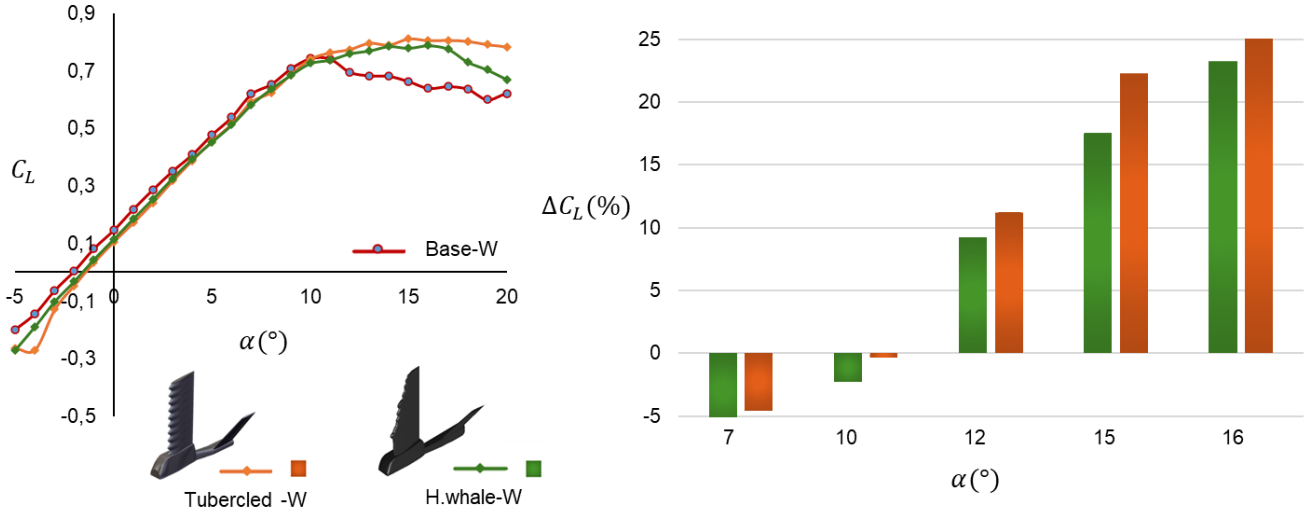



Figure 6 – Lift coefficient vs. angle of attack (left) and percentage variation of lift coefficient (right).

## 4.2 Drag coefficient

Regarding the drag coefficient, the three configurations present relatively similar values throughout the entire range of angles of attack analysed. Nevertheless, important differences can be observed depending on the operating regime (see Figure 7).

At low angles of attack, especially below $10°$, the conventional configuration (Eppler 186) provides the lowest drag values. This behaviour is expected, since the conventional wing has a cleaner leading-edge geometry and therefore generates lower drag under attached-flow conditions. Around cruise phase, angle of attack of $0°$, the humpback whale-inspired wing shows an approximate drag coefficient increase of 7% compared with the conventional wing. In the case of the constant tubercled wing, this increase is higher, reaching approximately 15%.

As the angle of attack increases and approaches the stall regime of the conventional wing, the drag differences between the configurations are partially reduced. For the humpback whale-inspired wing, the drag increase with respect to the conventional configuration decreases to approximately 4% near $10°$. In contrast, for the constant tubercled wing configuration, the aerodynamic drag increase remains close to 15%.

Once the stall angle of the conventional wing is exceeded, the drag coefficient of this configuration increases more sharply. In this range, the bioinspired configurations begin to show a more favourable behaviour. For angles of attack above $10°$, the realistic humpback whale-inspired configuration shows a drag reduction of approximately 10% compared with the conventional wing. In the case of the

constant tubercled wing, the reduction is more moderate, approximately 3%.

This drag reduction is maintained until the stall angles of the bioinspired wings are reached, which occur approximately between $15°$and $16°$.

This result is particularly relevant because, in the range of angles between approximately $10°$ and $15° - 16°$, the bioinspired configurations not only generate higher lift coefficient than the conventional wing, but may also present lower drag. This suggests a significant improvement in aerodynamic behaviour at high angles of attack.

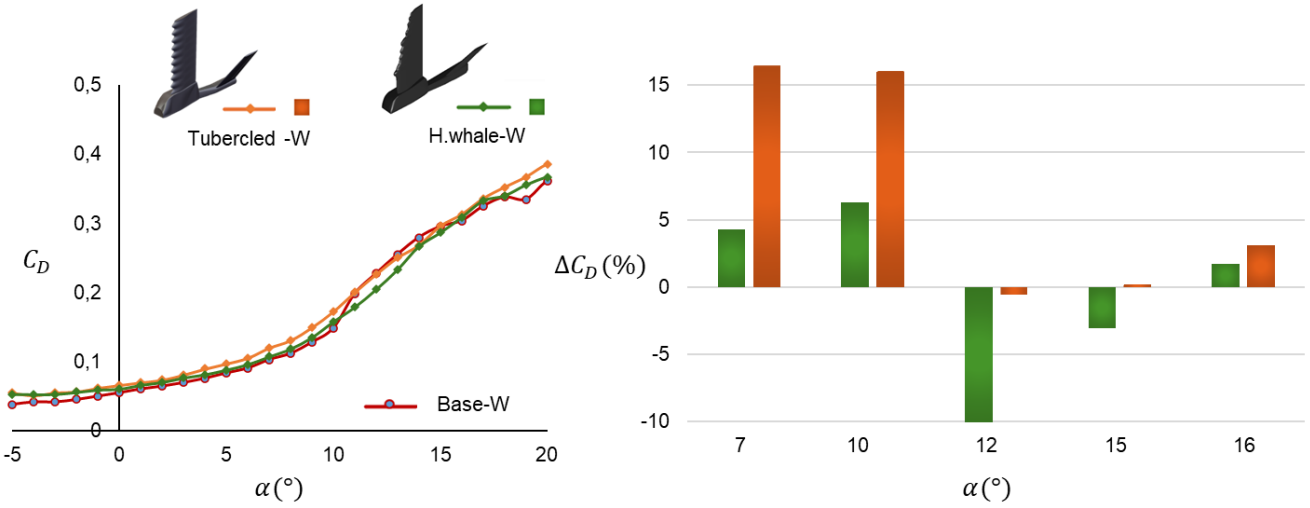



Figure 7 – Drag coefficient vs. angle of attack (left) and percentage variation of drag coefficient (right).

## 4.3 Aerodynamic efficiency

The aerodynamic efficiency $E$, expressed as the lift-to-drag ratio, $\frac{C_L}{C_D}$ allows the ability of the wing to generate lift with the lowest posible aerodynamic drag penalty to be evaluated (see Figure 8).

At low angles of attack, the conventional configuration (Eppler 186) clearly presents the highest aerodynamic efficiency values. This result is consistent with the previous analysis: in this regime, the conventional wing combines higher $C_L$ values with lower $C_D$ values, especially before the Flow separation (stall condition). However, once the stall angle of the conventional wing is exceeded, the trend changes notably. From approximately $10°$ onwards, the bioinspired configurations begin to show higher aerodynamic efficiency, since they maintain higher lift levels while avoiding the sharp drag increase associated with the stall of the conventional wing.

At an angle of attack of $12°$, the humpback whale-inspired configuration shows an increase in aerodynamic efficiency of approximately 20 % compared to the conventional wing. Ont he other hand, the constant tubercled configuration shows an improvement of approximately 11 %.

For higher angles of attack, both bioinspired wings maintain aerodynamic efficiency increases of around 20 % compared to the base wing (conventional). This confirms that the main advantage of tubercles geometry is not found in the low-angle-of-attack regime, but rather in conditions close to stall or beyond the stall of the conventional wing.

The experimental data show that the conventional configuration (Eppler 186 airfoil) offers the best aerodynamic performance at low angles of attack, where the flow remains attached and the aerodynamic drag penalty is minimal. In this regime, the conventional wing provides higher lift values and greater aerodynamic efficiency.

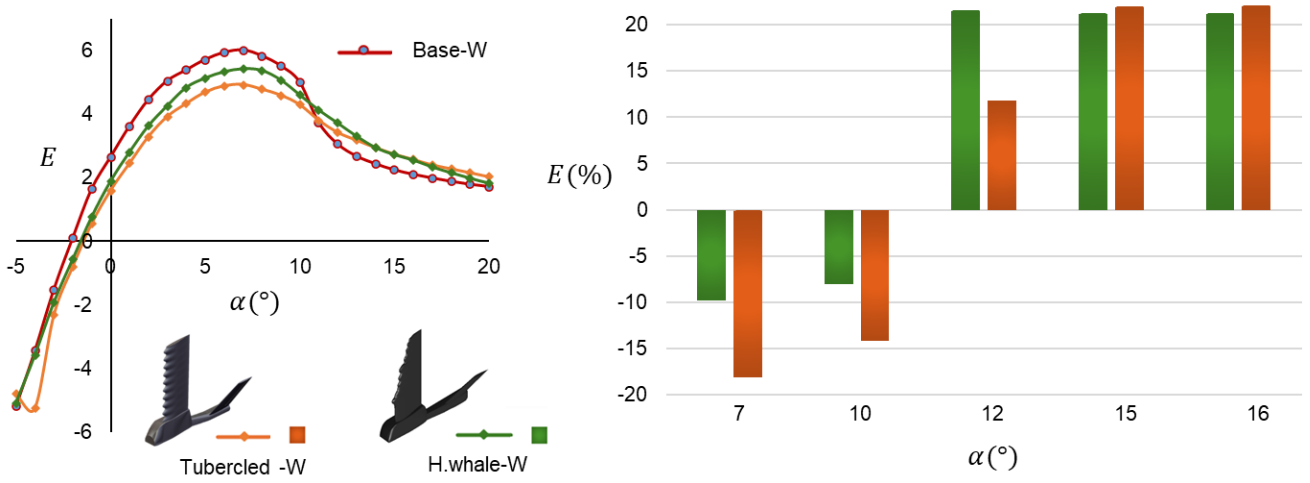



Figure 8 – Aerodynamic efficiency vs. angle of attack (left) and percentage variation of aerodynamic efficiency (right).

Nevertheless, the bioinspired configurations exhibit highly competitive behaviour. Although at low angles of attack they generate slightly lower lift and somewhat higher aerodynamic drag, the differences with respect to the conventional wing decrease as the angle of attack increases.

The main advantage of the tubercled configurations appears in the high-angle-of-attack regime. In this range, the tubercles modify the flow behaviour over the wing, delaying global flow separation and allowing high lift levels to be maintained for longer. As a result, stall is delayed by approximately 5 to 6 degrees compared to the base wing.

From an operational point of view, this behaviour is especially interesting for a small RPA, since it can improve the safety and stability of the vehicle during low-speed manoeuvres, high-angle-of-attack flight, take-off, landing, or conditions close to stall.

Furthermore, between $10°$ and $15° - 16°$, the bioinspired configurations combine an increase in lift coefficient with a relative reduction in aerodynamic drag compared to the conventional wing. This results in an improvement in aerodynamic efficiency within this operating range.

## 5. Conclusions

Based on the analysis of the experimental data, several conclusions can be drawn regarding the aerodynamic influence of leading-edge tubercles on small RPAS wings.

The conventional configuration (rectangular wing) provides the best aerodynamic performance at low angles of attack. In this regime, where the flow remains mostly attached, this wing shows higher $C_L$ values, lower $C_D$ values, and consequently greater aerodynamic efficiency than the bioinspired configurations. In particular, at $0°$, representative of cruise conditions, the lift coefficient of the conventional wing is approximately 20 % higher than that obtained with the bioinspired wings. Moreover, the bioinspired configurations present a drag penalty at low angles of attack, with an increase of approximately 7 % for the realistic humpback whale-inspired wing and approximately 15 % for the constant tubercled wing.

However, this advantage progressively decreases as the angle of attack increases. Between approximately $5°$and $7°$, the lift difference between the conventional and bioinspired configurations is reduced to around 5 %, while between $7°$ and $10°$, it decreases to approximately 2 – 3%. The conventional wing reaches its maximum lift coefficient, $C_{L,\max} \approx 0.74$, at around $10°$. Beyond this angle, stall occurs and a degradation of the lift coefficient is observed.

The main advantage of the bioinspired configurations appears at high angles of attack. Both the

humpback whale-inspired wing and the constant tubercled wing significantly delay stall, extending the operational range of the wing. The constant tubercled configuration delays stall up to approximately $15°$, corresponding to an improvement of about 5 degrees compared with the baseline wing. The realistic humpback whale-inspired configuration delays stall up to approximately $16°$, representing an improvement of about 6 degrees. This confirms that leading-edge tubercles can help maintain attached flow over a wider range of angles of attack and improve the stall tolerance of the wing.

Regarding lift generation, both bioinspired configurations outperform the conventional wing once the stall angle of the base configuration is exceeded. At $12°$, the constant tubercled wing provides an increase in lift coefficient of approximately 11 %, while the realistic humpback whale-inspired configuration increases $C_L$ by approximately 9 % compared with the base wing. At higher angles of attack, the lift improvement becomes even more significant, reaching values between approximately 17 % and 25 %. The constant tubercled wing generally reaches slightly higher lift coefficient values than the realistic configuration in this high-angle-of-attack range.

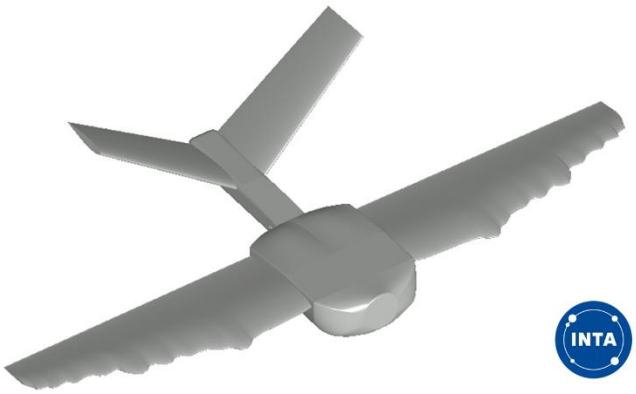



Figure 9 – Small RPA prototype with the realistic humpback tubercles.

Nevertheless, the humpback whale-inspired configuration presents a particularly interesting behavior from the point of view of aerodynamic drag. Although both bioinspired wings increase drag at low angles of attack, the realistic configuration shows a lower drag penalty than the constant tubercled wing. Furthermore, once the conventional wing has entered stall, the realistic humpback whale-inspired configuration provides a drag reduction of approximately 10 % compared with the base wing, whereas the constant tubercled configuration shows a more moderate reduction of approximately 3 %.

As a result of the combined increase in lift and the more favorable drag behavior, the aerodynamic efficiency of the bioinspired configurations improves significantly near and beyond the stall angle of the conventional wing. At $12°$, the realistic humpback whale-inspired wing increases the lift-to-drag ratio by approximately 20 % compared with the base configuration, while the constant tubercled wing provides an improvement of approximately 11 %. For higher angles of attack, both bioinspired wings maintain efficiency improvements of around 20 % relative to the conventional wing.

Overall, the results indicate that bioinspired wings can compete with the conventional configuration in the pre-stall regime and clearly outperform it under high-angle-of-attack conditions. This improvement translates into a greater stall margin, improved lift capability under critical conditions, and enhanced aerodynamic efficiency in regimes where the conventional wing loses performance. Therefore, the incorporation of leading-edge tubercles represents a promising passive flow-control solution to improve the aerodynamic characteristics of small RPAS, especially when the objective is to increase stall tolerance and improve vehicle behavior during low-speed flight, take-off, landing, gust encounters, or high-angle-of-attack maneuvers.

## Copyright Statement

The authors confirm that they, and/or their company or organization, hold copyright on all of the original material included in this paper. The authors also confirm that they have obtained permission, from the copyright holder of any third party material included in this paper, to publish it as part of their paper. The authors confirm that they give permission, or have obtained permission from the copyright holder of this paper, for the publication and distribution of this paper as part of the ICAS proceedings or as individual off-prints from the proceedings.

## References

[1] Fish, F. E., & Battle, J. M. (1995). Hydrodynamic design of the humpback whale flipper. Journal of Morphology, 225, 51–60.

[2] Fish, F. E., & Lauder, G. V. (2006). Passive and active flow control by swimming fishes and mammals. Annual Review of Fluid Mechanics, 38, 193–224.

[3] Fish, F. E., Weber, P. W., Murray, M. M., & Howle, L. E. (2011). The tubercles on humpback whales' flippers: Application of bio-inspired technology. Integrative and Comparative Biology, 51(1), 203–213.

[4] New, D. T. H., & Ng, B. F. (Eds.). (2020). Flow Control Through Bio-inspired Leading-Edge Tubercles: Morphology, Aerodynamics, Hydrodynamics and Applications. Springer.

[5] Miklosovic, D. S., Murray, M. M., Howle, L. E., & Fish, F. E. (2004). Leading-edge tubercles delay stall on humpback whale flippers. Physics of Fluids, 16, L39–L42.

[6] Johari, H., Henoch, C., Custodio, D., & Levshin, A. (2007). Effects of leading-edge protuberances on airfoil performance. AIAA Journal, 45(11), 2634–2642.

[7] Hansen, K. L., Kelso, R. M., & Dally, B. B. (2011). Performance variations of leading-edge tubercles for distinct airfoil profiles. AIAA Journal, 49(1), 185–194.

[8] Zhang, M. M., Wang, G. F., & Xu, J. Z. (2013). Aerodynamic control of low-Reynolds-number airfoil with leading-edge protuberances. AIAA Journal, 51(8), 1960–1971.

[9] Rostamzadeh, N., Hansen, K. L., Kelso, R. M., & Dally, B. B. (2014). The formation mechanism and impact of streamwise vortices on NACA 0021 airfoil's performance with undulating leading edge modification. Physics of Fluids, 26, 107101.

[10] Ni, Z., Su, T. C., & Dhanak, M. (2018). An empirically-based model for the lift coefficients of twisted airfoils with leading-edge tubercles. AIP Advances, 8, 045123.

[11] Moscato, G., Mohamed, J., & Romano, G. P. (2022). Improving performances of biomimetic wings with leading-edge tubercles. Experiments in Fluids, 63, 146.

[12] Sudhakar, S., Karthikeyan, N., & Venkatakrishnan, L. (2017). Influence of leading edge tubercles on aerodynamic characteristics of a high aspect-ratio UAV. Aerospace Science and Technology, 69, 281–289.

[13] Sudhakar, S., & Karthikeyan, N. (2013). Effect of leading edge tubercles on flow field over NACA-4415 airfoil at low Reynolds number. 14th Asian Congress of Fluid Mechanics, Hanoi and Halong, Vietnam.

[14] Bardera, R., Rodríguez-Sevillano, Á. A., Barroso-Barderas, E., & Matías-García, J. C. (2024). CFD study of the effect of leading-edge tubercles on the aerodynamic characteristics of a small UAV based on Eppler 186 airfoils. Results in Engineering.

[15] Wei, Z., New, T. H., & Cui, Y. D. (2018). Aerodynamic performance and surface flow structures of leading-edge tubercled tapered swept-back wings. AIAA Journal, 56(1), 423–431.

[16] Murray, M. M., Miklosovic, D. S., Fish, F. E., & Howle, L. E. The effects of tubercles on swept wing performance

[17] Seyhan, M., Akbıyık, H., Sarıoğlu, M., & Keçecioğlu, S. C. (2022). The effect of leading-edge tubercle on a tapered swept-back SD7032 airfoil at a low Reynolds number. Ocean Engineering, 266, 112794

[18] Custodio, D. (2007). The effect of humpback whale-like leading edge protuberances on hydrofoil performance. Master's Thesis, Worcester Polytechnic Institute.

[19] Weber, P. W., Howle, L. E., Murray, M. M., & Fish, F. E. (2011). Lift, drag, and cavitation onset on rudders with leading-edge tubercles. Marine Technology and SNAME News, 48(1), 27–36.

[20] Li, J., Liu, C., & Li, X. (2021). Effects of wavy leading-edge protuberance on hydrofoil performance and its flow mechanism. Journal of Marine Science and Engineering, 9, 1138.